



A New Consensus-based Distributed Adaptive Control for Islanded Microgrids

M. Keshavarz^a, A. Doroudi^{*a}, M. H. Kazemi^a, N. Mahdian Dehkordi^b

^a Electrical Engineering Department, Shahed University, Tehran, Iran

^b Control Department of Electrical Engineering Faculty, Shahid Rajaee Teacher Training University, Tehran, Iran

PAPER INFO

Paper history:

Received 15 March 2021

Received in revised form 21 April 2021

Accepted 04 June 2021

Keywords:

Adaptive Control

Distributed Control

Consensus Protocol

Disturbances

Microgrids

Secondary Control

ABSTRACT

This paper proposes a novel distributed adaptive secondary controller for microgrids (MGs) in islanded operation. To enhance the dynamic behaviour of a microgrid considering uncertainties and disturbances, the proposed controller uses a consensus-based adaptive control structure. A novel consensus protocol is proposed to restore the frequency and voltage (f & V) of a microgrid to their rated values. A Lyapunov function is presented to assure the asymptotic stability of the controller and the ultimate boundedness of the global neighborhood consensus error. The nonlinear nature of MGs has been also considered in the algorithm. Unlike other methods in this field that require complete information of distributed generators (DGs), the proposed controller requires only power droop coefficients and is independent of DGs parameters. Different simulations are conducted in MATLAB/SimPower Toolbox on a typical microgrid and under various disturbances to judge the performance of the adaptive controller. The simulation results show the effect of the proposed controller on increasing the resilience of an MG.

doi: 10.5829/ije.2021.34.07a.17

NOMENCLATURE

Z_{oi}	Avirtual signal	f_i, k_i, g_i, h_i	Nonlinear Functions
D_i	An Uncertainty	a, b	Nonnegative Real Number
V_{ref}	DG Output Voltage	i^{th}	Receiving Node
DG	Distributed Generator	j^{th}	Sending Node
DAFC	Distributed Adaptive Frequency Controller	L	Laplacian Matrix
DSC	Distributed Secondary Control	$u_i = [\tau_i \ \varpi_i]$	Output Of Secondary Controller
DVAC	Distributed Adaptive Voltage Controller	G	Pinning Matrix
D_{Pi}, D_{Qi}	Droop Coefficients	p, q	Positive Numbers
ξ_{oi}	Frequency Consensus Error	P_i, Q_i	Output Real and Reactive Powers
$f \& V$	Frequency and Voltage	ξ_{Pi}	Real Power Neighbors Tracking Error
ξ_{vi}	local Neighborhood Consensus Error	SCL	Secondary Control Layer
MG	Microgrid	τ_i, ϖ_i	Set Points
λ_0	Minimum Eigenvalue	β	Steady State Error
σ_{min}	Minimum Singular Value	VSC	Voltage Source Converter
Z_{oi}	Avirtual signal	f_i, k_i, g_i, h_i	Nonlinear Functions
D_i	An Uncertainty	i^{th}	Receiving Node
V_{ref}	DG Output Voltage		

*Corresponding Author Institutional Email: doroudi@shahed.ac.ir

(A. Doroudi)

1. INTRODUCTION

Currently, renewable energy sources have a significant share of modern power networks [1]. MG is a cluster of small power networks made of several renewable energy sources (photovoltaics, wind turbines, micro-turbines, etc.), energy storage units and, electrical loads [1-2]. MGs can operate in both grid-connected and islanded operating modes. In grid-connected mode, the main grid directly control the frequency and voltage (f & V) of MG, whereas, in islanded mode, all DGs are responsible to maintain these quantities within pre-specified limits [2, 3]. Proper control of microgrid is a prerequisite for stable and economically efficient operation [4,5]. To maximize the use of resources and improve the effectiveness of DGs, a modern control approach is required to increase the microgrid reliability and to provide global stability for the system [6, 7].

In general, the MGs control system is carried out at three levels of hierarchy including primary, secondary, and tertiary control levels [7]. The primary control level is related to the local control loops along with droop control of the DGs without requirements for the communication infrastructure. It stabilizes the microgrid f & V and shares the active and reactive power between individual DG units using local current, voltage, and, droop power control loops [8, 9]. The main drawback of this control scheme is the steady-state f & V deviations from their reference values. The secondary control layer (SCL) is utilized to overcome this drawback and compensate for f & V deviations result from the droop control method. The SCL can be implemented in three manners: centralized [10-12], decentralized [13, 14], and distributed [15-21]. The centralized control method employs a central control module and a communication grid between each DG and the central controller. Therefore, it demands extensive communication system to collect and process the massive information of all DGs. As a result, this control method suffers from the drawbacks of the presence of a single point of failure and low reliability [10]. The decentralized control strategy is not usually employed in the secondary control due to the lack of sufficient information to coordinate and harmonize all available MGs resources [13, 14]. To overcome the centralized and decentralized controls problems, inspired by the idea of multi-agent systems, distributed control methods using sparse communication networks have been recently presented [15-21]. In the distributed control scheme, each agent only communicates with the neighboring agents employing a sparse communication grid. The control method reduces the communication grid complexity and is needless of a central controller, and consequently enhance the overall microgrid reliability [22-26]. The third and highest level of control system structure is the tertiary control and essentially deals with economic dispatch and optimal

power flow [27].

So far, different types of distributed secondary control (DSC) algorithms have been developed [22-25]. Thanks to the graph theory, consensus protocol is the base of the great number of these algorithms [20,21]. In multi-agent systems, reaching an agreement on a certain amount that depends on the status of all agents is called consensus. When each DG is considered as an agent, returning f & V to the reference values (synchronization process) can be a matter of consensus. Distributed synchronization process necessitates that each agent (i.e., each DG) exchange information with other agents by a consensus protocol. A DSC scheme for islanded microgrids is presented by Dehkordi et al. [25]. Two individual f & V controllers are separately designed and examined. A distributed finite-time approach is first proposed to ensure the finite time restoration of voltage magnitude. The frequency restoration algorithm is then presented so that correct real power sharing is achieved. A two-layer DSC protocol is proposed by Bidram et al. [28]. Voltage source inverters (VSIs) are utilized in the first layer for maintaining f & V of the microgrid. The second layer which consists of current source inverters (CSIs) shares the reactive and active powers among DGs in an appropriate manner. The effects of delays and noises in communication channels among DGs have been discussed by Shahab et al. [29] thorough stochastic and/or distributed time-delay control methods. Moreover, detail discussion about communication delays' effect on the control of an islanded MG has been investigated by a small-signal model in literature [10,18]. A distributed voltage averaging method was proposed by Amoateng et al. [22] to provide a simple compromise between the incompatible objectives of bus voltages regulating and good reactive power sharing.

A novel DSC approach is proposed by Bidram et al. [30]. The proposed approach is fully distributed and its structure needs a sparse communication grid. To transform the secondary voltage control to a linear synchronization problem, input-output feedback linearization technique was employed. Anyway, the control method is so complex and heavily depends on DGs parameters and network dynamics. Multi-functional DSC structure was proposed by Li et al. [31] with individual frequency, voltage and active power regulator modules. The method, however, needs normalized power information of all DGs.

Microgrid along with its control system is an unknown nonlinear and time-variable system and always prone to uncertainties which are caused by internal disturbances such as parametric variations and unmodeled dynamics or external disturbances such as load changes and DG tripping events [29-32]. Currently to face these challenges, the development of model-free distributed adaptive controllers has become the focus of researchers. Bidram and Davoudi [33] proposed an

adaptive secondary voltage control scheme for microgrids in islanded mode. The paper has used the input output feedback linearization technique like [29] to achieve a linear dynamic system. The fault tolerant consensus-based control of multi agent systems, when the faults and disturbances coexist, have recently been presented in the literature to control multi-agent systems [34]. Anyway, the control method is very complex and heavily depends on DGs parameters and network dynamics. A new cooperative adaptive distributed consensus protocol was presented in the presence of unmodated dynamics by Amoateng et al. [22]. To achieve this goal, a smart secondary adaptive control protocol is proposed which uses two neural networks based identifier and controllers. High computational complexity, knowing DGs information for training neural networks and, need for a specially designed switching scheme between the two controllers are the three disadvantages of this method. Dehkordi et al. [27] proposed a fully DSC to restore f & V , irrespective of parametric uncertainties. However, the paper still needs DGs parameters.

In this paper, a new adaptive fully DSC is proposed. The MG system is considered as an unknown nonlinear dynamic system. A Novel control scheme as a consensus problem is introduced and a Lyapunov proof is presented to assure the asymptotic stability of the control system. The upper bound of the consensus error is also explicitly derived. The proposed controller covers the uncertain dynamics and nonlinear nature of MGs and requires only active and reactive droop coefficients. The followings are the main novelty of the paper:

- a. The proposed adaptive protocol is fully distributed and ensures MG asymptotic stability.
- b. The goal of any controller design is to maintain system performance despite of inaccuracies and model changes. The proposed adaptive protocol is less dependent on system parameters and DGs than existing distributed adaptive control methods.
- c. The proposed secondary controller is adaptive and robust and it can easily respond to severe uncertainties such as communication link failures and DG outages.

The reminder of this paper is structured as follows: section 2 presents the modeling approach. The proposed Algorithm is presented in section 3. In section 4, simulation results are discussed and finally, conclusions are summarized in sections 5.

2. MODELING APPROACH

2.1. Preliminaries of Graph Theory A rooted-out branching (directed tree) topology is commonly assigned as a sparse communication network for microgrid systems. In this topology (Figure 1), DGs are

considered as the nodes of the communication digraph and the edges denote the communication links. Each edge establishes a connection between a pair of nodes, and each node receives information, only from one node (except the root node). In fact, the information exchange among DGs is done on a directed graph $G = (v, \varepsilon, A)$ that consists of N nodes called $v = (1, 2, \dots, N)$, a set of link ε , and its associated adjacent matrix $A(N \times N)$. a_{ij} is the weight of edge (v_j, v_i) . For $a_{ij} = 1$, i^{th} node receives information from j^{th} node, otherwise $a_{ij} = 0$.

The Laplacian matrix L is assigned as $L_{ii} = \sum_{j=1}^N a_{ij}$ and $L_{ij} = -a_{ij}$. The eigenvalues of L has one zero entry ($\lambda_1 = 0$) with all other have positive real parts, i.e., $0 \leq \lambda_2 \leq \lambda_3 \leq \dots \leq \lambda_N$ [25].

It is noteworthy that in the proposed control strategy, any type of directed graph (digraph) can be employed and the only necessary condition for the selected digraph is to have a spanning tree. If there is a directed path between the root node and any other node in a digraph, the digraph will actually have a spanning tree.

2.2. Modeling of MGs Figure 2 shows an islanded MG depicting its power network, communication grid, and control layers. The power network interconnects the primary DC source to the voltage source converter (VSC) including power, voltage, and current control loops. VSC is connected to the network thorough an LCL filter. The primary control loops regulate the desired outputs of the inverter bridge. D-q reference frame is utilized to formulate the nonlinear dynamics of the system [30].

Frequency and voltage values must be readjusted after any disruption. The local droop method is adopted to balance the generation and consumption of active and reactive power. A relationship between the active power and frequency and the voltage amplitude and reactive power is assigned by the power controller block as follows:

$$\omega_i = \varpi_i - D_{P_i} P_i \tag{1}$$

$$v_{odi} = \mathfrak{X}_i - D_{Q_i} Q_i, v_{oqi} = 0 \tag{2}$$

where P_i and Q_i are the measured real and reactive power at DG output, respectively. τ_i and ϖ_i are the set points and D_{P_i} and D_{Q_i} are the droop coefficients.

A microgrid has a nonlinear nature and resembles a multiagent system. In distributed control structure, each

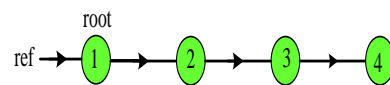


Figure 1. Topology of the communication graph

DG communicates with its neighbor units through a communication grid. The nonlinear dynamics of the i^{th} DG can be written as Equation (3) in state equations form:

$$\begin{cases} \dot{x}_i = f_i(x_i) + k_i(x_i)D_i + g_i(x_i) u_i \\ y_i = h_i(x_i) \end{cases} \quad i=0,\dots,N \quad (3)$$

Details of DG and its components equations are given in literature [33]. D_i is considered as an uncertainty. $u_i = [\tau_i \ \omega_i]$ is the output of secondary controllers. They are assigned such that f & V of all DGs regulated to the reference values. f_i , k_i , g_i and h_i are nonlinear functions.

So far, two types of methods have been proposed to design an adaptive secondary control for a microgrid modeled with nonlinear Equation (3). In the first type, neural networks are used instead of nonlinear model. In order to train these networks, the microgrid information must be available. In the second type, input–output feedback linearization technique is utilized to transform the nonlinear dynamics into the linear form. This technique needs $f_i(x_i)$, $g_i(x_i)$ and their derivative to x_i for the design and implementation of the distributed secondary controller. Hence, they have high dependence on the system and DGs parameters.

In this paper, the modelling of the MG system is performed in the form of an unknown nonlinear dynamic system. However, having active and reactive droop coefficients of DGs is sufficient to ensure the synchronization process. The controller protocol only requires the measured output signals of the DGs and there is no need to modify the controller parameters if there exists inaccuracies or changes in the power network

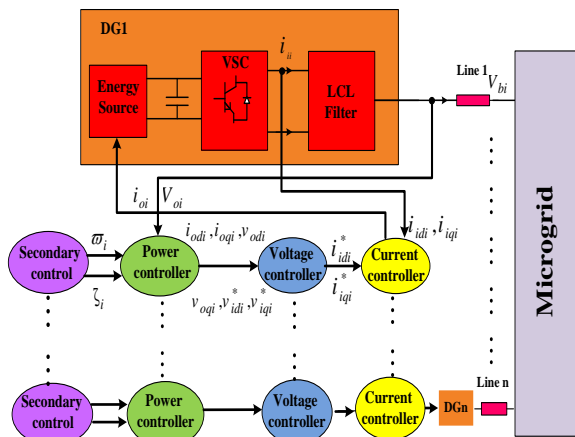


Figure 2. Schematic diagram of a MG including inverter-based DGs with their primary and secondary controllers

parameters. The set point for primary control is provided by secondary controller. The secondary control also restores the outputs of individual DG units to a reference value by the communication network that shares information among DGs.

3. PROPOSED ALGORITHM

3. 1. Distributed Adaptive Voltage Controller (DAVC)

This section aims to develop a novel consensus based DAVC for microgrids in islanded mode. DAVC is responsible for elimination of the voltage deviations caused by primary droop mechanism. The compact form of secondary voltage control equations can be written as Equation (2). Differentiating these equation yields:

$$\dot{v}_{odi} = \tilde{x}_i - D_{Qi}\dot{Q}_i \equiv Z_{vi} \quad (4)$$

DAVC should guarantee that the DG output voltage magnitudes all synchronises with V_{ref} . The proposed adaptive control law is as follows:

$$\begin{aligned} Z_{vi} &= -(d_{vi} + \rho_{vi})\xi_{vi} \\ \dot{\xi}_{vi} &= \xi_{vi}^T \xi_{vi}, \quad \rho_{vi} = \xi_{vi}^T \xi_{vi} \end{aligned} \quad (5)$$

where ξ_{vi} is the local neighborhood consensus error:

$$\xi_{vi} = \sum_{j=1}^N \tilde{L}_{ij}(v_{odi} - v_{odj}) + G_{ij}(v_{odi} - v_{ref}) = \sum_{j=1}^N \tilde{L}_{ij}(v_{odi} - v_{ref}) \quad (6)$$

G is a diagonal matrix and called the pinning matrix. The pinning gain (the diagonal element of the pinning matrix) is nonzero only for the nodes that are directly connected to the root (leader) node. The nodes for which the pinning gain is nonzero are referred to as the pinned or controlled nodes.

In matrix form, Equation (6) may be given as:

$$\xi_v = (L + G)\varepsilon_v = \tilde{L}\varepsilon_v \quad (7)$$

It is easy to prove that [35]:

$$\|\varepsilon_v\| \leq \frac{\|\xi_v\|}{\sigma_{\min}(\tilde{L})} \quad (8)$$

$\sigma_{\min}(\tilde{L})$ depicts the minimum singular value of matrix \tilde{L} . In multi-agent systems the main problem is the definition of a consensus protocol. The protocol describes the rules by which each agent interacts with its neighboring agents so that all agents can reach the desired state.

Figure 3 shows a rooted-tree graph with 6 nodes used in this paper. Each node (except the root node) takes information from its neighbor and sends it to the next node. The numbers shown on the links are the contribution of the state of each node to the next node.

As the root node is the only pinned node in Figure 3, all elements of G are zero except the first element which is one. Therefore, \tilde{L} is as follows:

$$\tilde{L} = \begin{bmatrix} 1 & 0 & 0 & 0 & \dots & 0 & 0 \\ -1 & 1 & 0 & 0 & \dots & 0 & 0 \\ \vdots & \vdots & \vdots & \vdots & \ddots & \vdots & \vdots \\ 0 & 0 & 0 & \dots & -1 & 1 & 0 \\ 0 & 0 & 0 & \dots & 0 & -1 & 1 \end{bmatrix} \quad (9)$$

From Equation (6), we have:

$$\dot{\xi}_{vi} = \tilde{L}\dot{\varepsilon}_{vi} = \tilde{L}\dot{v}_{odi} = \tilde{L}Z_{vi} \quad (10)$$

Let the Lyapunov function candidate is [36]:

$$V = \sum_{i=1}^N \frac{1}{2} m_i (2d_{vi} + \rho_{vi}) \rho_{vi} + \sum_{i=1}^N \frac{1}{2} m_i (d_{vi} - \beta)^2 \quad (11)$$

where $m_i \geq 0$ are the diagonal elements of a diagonal matrix M . The derivative of Lyapunov function is:

$$\begin{aligned} \dot{V} &= \sum_{i=1}^N (m_i \dot{d}_{vi} \rho_{vi} + m_i \dot{\rho}_{vi} d_{vi} + m_i \dot{\rho}_{vi} \rho_{vi}) + \sum_{i=1}^N m_i (d_{vi} - \beta) \dot{d}_{vi} \\ &= \sum_{i=1}^N m_i (d_{vi} + \rho_{vi}) \dot{\rho}_{vi} + m_i (d_{vi} + \rho_{vi} - \beta) \dot{d}_{vi} \end{aligned} \quad (12)$$

The matrix form of Equation (12) can be written as:

$$\dot{V} = (D + \rho)M\dot{\rho} + (D + \rho - \beta)M\dot{D} \quad (13)$$

By substituting Equation (5) into Equation (13), we have:

$$\begin{aligned} \dot{V} &= 2(D + \rho)M\xi_v^T \dot{\xi}_v + (D + \rho - \beta)M\xi_v^T \dot{\xi}_v \\ &= 2\xi_v^T (D + \rho)M\dot{\xi}_v + \xi_v^T (D + \rho - \beta)M\dot{\xi}_v \end{aligned} \quad (14)$$

Placing $\dot{\xi}$ from Equation (10) into Equation (14) yields:

$$\dot{V} = 2\xi_v^T [-(D + \rho)^2 M\tilde{L}] \xi_v + \xi_v^T [(D + \rho - \beta)M] \xi_v \quad (15)$$

$M\tilde{L}$ can be written as $\frac{1}{2}(M\tilde{L} + \tilde{L}^T M)$ [37, 38]. Then:

$$\begin{aligned} \dot{V} &= \xi_v^T [-(D + \rho)^2 (M\tilde{L} + \tilde{L}^T M) + (D + \rho - \beta)M] \xi_v \\ \dot{V} &\leq \xi_v^T [-\lambda_0 (D + \rho)^2 + (D + \rho)M - \beta M] \xi_v \end{aligned} \quad (16)$$

where λ_0 is the minimum eigenvalue of $(M\tilde{L} + \tilde{L}^T M)$. Lemma 1 [39]: If a and b are nonnegative real number and p and q are positive numbers such that $\frac{1}{p} + \frac{1}{q} = 1$,

$$ab \leq \frac{a^p}{p} + \frac{b^q}{q}$$

then By applying Lemma 1 and assumed that $a = \sqrt{\lambda_0}(D + \rho)$, $b = \sqrt{\beta M}$, $p = q = 2$, Equation (16) can be written as:

$$\begin{aligned} \dot{V} &\leq \xi_v^T [-2\sqrt{\lambda_0\beta M}(D + \rho) + (D + \rho)M] \xi_v \\ \dot{V} &\leq \xi_v^T [(D + \rho)(M - 2\sqrt{\lambda_0\beta M})] \xi_v \end{aligned} \quad (17)$$

$$\beta \geq \frac{\max\{m_1, \dots, m_N\}}{\lambda_0}$$

Hence, if then $\dot{V} \leq 0$ and the proof is completed. Indeed, according to Equation (10),

β represents steady state error and qualifies the ultimate boundedness of consensus error.

Figure 4 shows the DVAC block diagram. The controller output τ_i could be written as:

$$\tau_i = \int (Z_{vi} + D_{Qi}\dot{Q}_i) dt \quad (18)$$

3. 2. Distributed Adaptive Frequency Controller (DAFC)

DAFC should assign ϖ_i in Equation (1) for synchronization of all DGs frequency. In fact, this controller simulates the governor and its set point mechanism from a synchronous generator. By differentiating of Equation (1), we have:

$$\dot{\omega}_i = \dot{\varpi}_i - D_{Pi}\dot{P}_i \equiv Z_{\omega i} \quad (19)$$

where $Z_{\omega i}$ is a virtual signal. As the frequency is a global quantity among a MG, the DAFC can be proposed in such a way that in addition to frequency synchronization, the sharing of DGs output real powers are divided according to their nominal (rated) powers. It means that:

$$\frac{P_j}{P_i} = \frac{D_{Pi}}{D_{Pj}}, \quad \forall i, j \in N \quad (20)$$

Similar to the previous section, the control law is introduced as follows:

$$Z_{\omega i} = -(d_{\omega i} + \rho_{\omega i})\xi_{\omega i} \quad (21)$$

where $\xi_{\omega i}$ is the frequency consensus error:

$$\xi_{\omega i} = \sum_{j=1}^N L_{ij}(\omega_i - \omega_j) + G_{ij}(\omega_i - \omega_{ref}) \quad (22)$$

ϖ_i is written as:

$$\varpi_i = \int (Z_{\omega i} + D_{Pi}\dot{P}_i) dt \quad (23)$$

For appropriate active power sharing, the following signal Z_{Pi} is introduced:

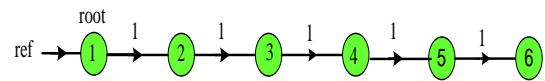


Figure 3. Topology of the communication grid with six nodes

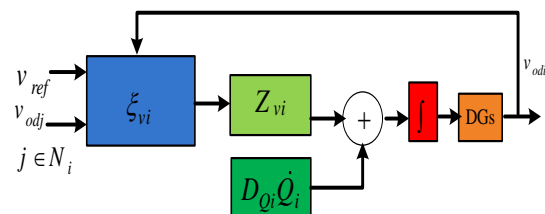


Figure 4. Schematic of the proposed DVAC

$$Z_{P_i} = -(d_{P_i} + \rho_{P_i})\xi_{P_i} \quad (24)$$

where ξ_{P_i} is the real power neighbors tracking error:

$$\xi_{P_i} = \sum_{j=1}^N a_{ij}(D_{P_i}P_i - D_{P_j}P_j) \quad (25)$$

Now, Equations (21) and (24) can be combined to design the ϖ_i as the controller output.

$$\varpi_i = \int (Z_{\omega_i} + Z_{P_i})dt \quad (26)$$

Figure 5 shows the DAFC block diagram.

4. SIMULATION RESULTS

An typical MG is used for demonstration the effectiveness of the proposed control strategy. For this purpose, A 50 Hz, 380 V, islanded microgrid with six DGs, five loads and several lines is considered (Figure 6). The communication topology is depicted in Figure 3. DG1 (the reference DG) is the only agent which accesses to the f & V reference values. The specifications of DGs, RL loads, transmission lines, and the control system are summarized in Table 1. MATLAB/SimPower software environment is used to test all the simulation scenarios.

It should be note that although the proposed distributed control method is analyzed by a 6-node microgrid, the design procedure is modular and scalable and can be implemented in larger microgrid with more DGs.

The results of the proposed control strategy are also compared with the data reported in literature [28], which is one of the main and last activities accomplished in this field. By doing this, better capabilities of the proposed method are represented in compare to the conventional distributed methods. Four different cases, with different degree of uncertainty and disturbance levels are used for evaluation the behavior of the proposed controllers.

4. 1. Case 1: Load Changes In this section, the behavior of the proposed method is investigated in response to the load change and compared with the method of Bidram et al. [28]. The following is the simulation scenario:

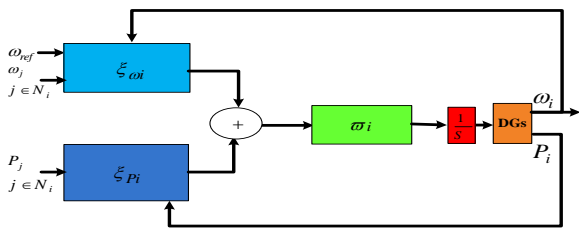


Figure 5. Schematic of the proposed DAFC

TABLE 1. Parameters of the test MG

		DG #1&2&5	DG #3&4&6
DGs	DP	1.06×10^{-4}	1.06×10^{-4}
	DQ	5.02×10^{-3}	5.02×10^{-3}
	Z_c	$0.015 + j0.65 \Omega$	$0.03 + j0.65 \Omega$
	L_{f1}, L_{f2}	1.35, 0.27mH	1.35, 0.27mH
	R_{f1}, R_{f2}	0.1, 0.05 Ω	0.1, 0.05 Ω
	C_f	47 μ F	47 μ F
	K_{pv}	0.1	0.05
	K_{IV}	420	390
Lines	Z_{line1}	$0.12 + j0.1 \Omega$	$0.175 + j0.58 \Omega$
	Z_{line2}	$0.175 + j0.58 \Omega$	$0.12 + j0.1 \Omega$
	Z_{line3}	$0.12 + j0.1 \Omega$	$0.175 + j0.58 \Omega$
	Z_{line4}	$0.12 + j0.1 \Omega$	$0.175 + j0.58 \Omega$
	Z_{line5}	$0.12 + j0.1 \Omega$	$0.175 + j0.58 \Omega$
	Z_{line6}	$0.175 + j0.58 \Omega$	$0.12 + j0.1 \Omega$
	Z_{line7}	$0.12 + j0.1 \Omega$	$0.175 + j0.58 \Omega$
	Z_{line8}	$0.12 + j0.1 \Omega$	$0.175 + j0.58 \Omega$
RL Loads	Load #1	P=13 kW, Q=7.5 kVar	Load #3 P=7 kW, Q=7 kVAR
	Load #2	P=13 kW, Q=7.5 kVar	Load #4 P=6 kW, Q=6 kVAR
	Load #5	P=14 kW, Q=6 kVar	

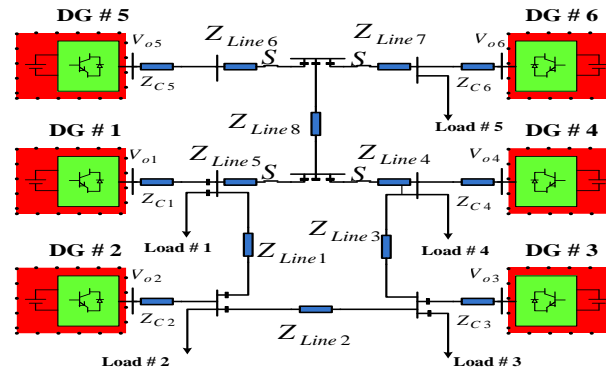


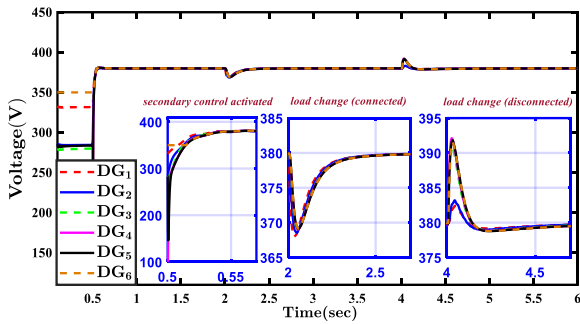
Figure 6. Isolated test MG

- 1) $t = 0$ s is the simulation starting time. The secondary controllers are off and only the primary control is working.
- 2) At $t = 0.5$ s, the secondary controllers are applied. It should be noted that in practical applications, the secondary voltage control should be applied immediately after the disturbance occurs. However, in this paper, the secondary controller is intentionally delayed by 0.5 s. to highlight its effectiveness.
- 3) At $t = 2$ s, a load with $P = 6$ kW and $Q = 6$ kVar is connected to the bus1 (parallel to the existing load).
- 4) At $t = 4$ s, loads 3 and 4 are disconnected from the MG.

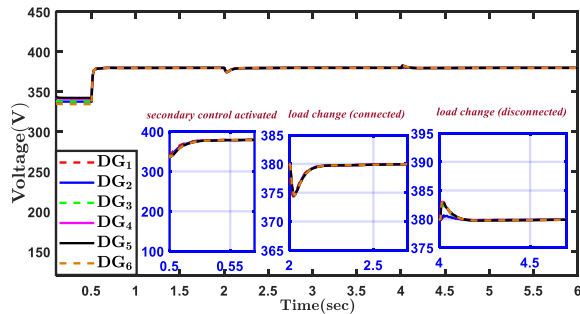
Figures 7a and (8a) show the voltage (frequency) of DGs deduced by the method of Bidram et al. [28] and Figures 7b and (8b) represent the voltage (frequency) of DGs obtained by the proposed method. As it can be seen in these figures, at the beginning and once the primary

control is applied, DGs operating f & V all go to a common values that deviate from the nominal values. After the secondary controllers are applied at $t = 0.5$ s, a short transient occurs and both f & V quickly return to their nominal values. Then, load changes occur at $t=2$ s and $t=4$ s. Transient periods are zoomed to show details that are not shown in the original figures. The zoomed regions show that both overshoot and settling time resulting from the proposed method are less than those parameters obtained from the method [28].

Figures 9a and 9b represent the output real power ratio of the six DGs using Bidram et al. [28] method and the proposed strategy, respectively. As shown, the proposed strategy presents appropriate real power sharing among all DGs.

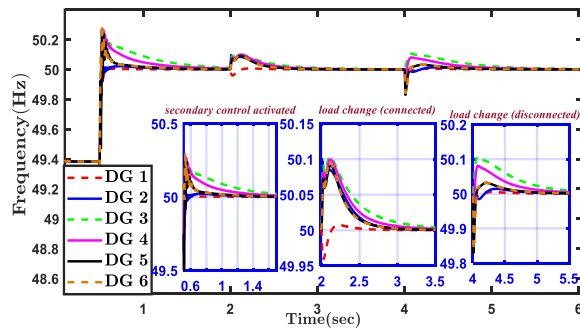


(a) method of Bidram et al. [28]

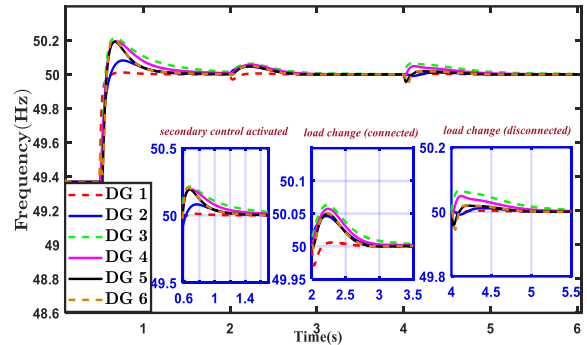


(b) the proposed method

Figure 7. DGs output voltage magnitudes

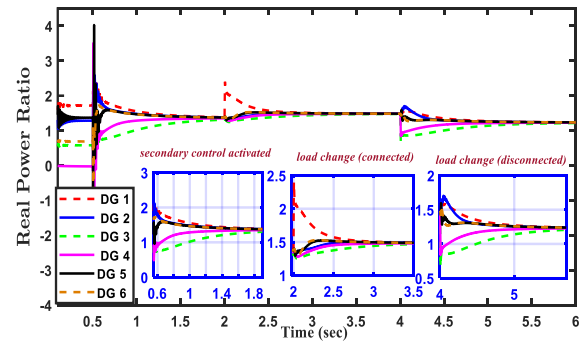


(a) method of Bidram et al. [28]

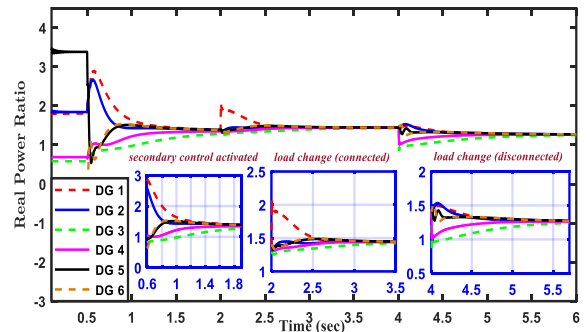


(b) the proposed method

Figure 8. DGs output frequency



(a) method of Bidram et al. [28]



(b) the proposed method

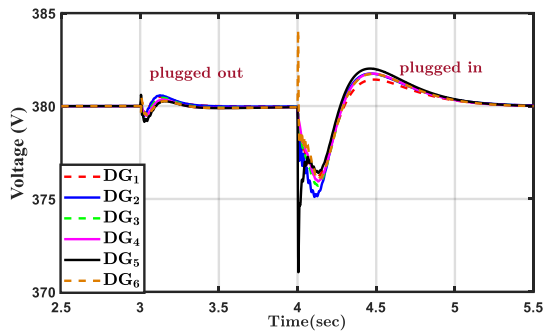
Figure 9. DGs output real power ratio

4. 2. Case 2: Plug and Play Capability

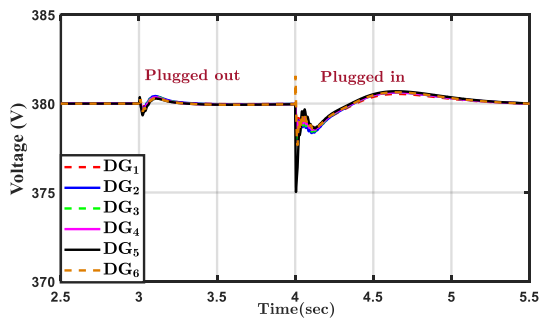
In this case, a higher disturbance level is assumed and the plug-and-play capability of the proposed controllers is investigated. For this purpose, at $t = 3$ s, DG 6 is unplugged from the MG and is plugged back in at $t = 4$ s. Although this DG is instantly turned off, the power measurements exponential decay to zero because of the existing low-pass filters. The control parameters are the same as in case 1. The results are displayed in Figures 10(a), 11(a) and 12(a) for method of Bidram et al. [28] and in Figures 10(b), 11(b) and 12(b) for the proposed method. As it is seen, the proposed controller responds well to the outage and reconnection of the DG unit, which

can be considered as a large disturbance. Also, the proposed controller maintains accurate proportional power sharing and frequency and voltage regulation before, during, and after the plug-and-play event with much less transients than those of Bidram et al. [28]. After unplugging of DG6 at $t=3$ s, the other units share the excess power among themselves in proportion to their power ratings. It should be noted that although DG 6 is disconnected from Bus 6, the bus voltage is still available.

4. 3. Case 3: Failure of Communication Links In this case, resiliency to a single link failure is investigated. It is assumed that at $t = 3$ s, the communication link between DG1 and DG2 is deliberately disconnected and reconnected after 1 m.s.

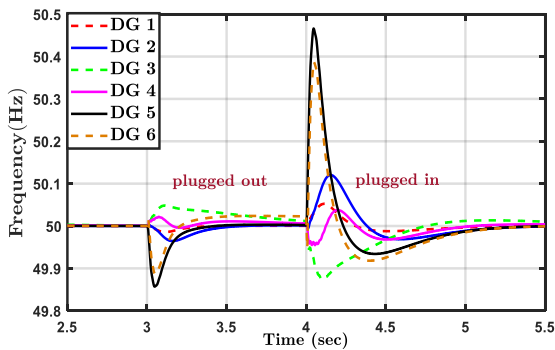


(a) method of Bidram et al. [28]

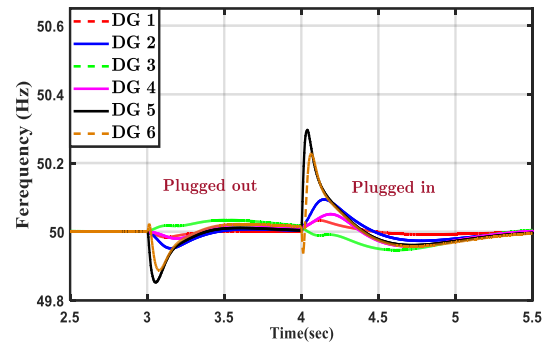


(b) the proposed method

Figure 10. DGs output voltage magnitudes

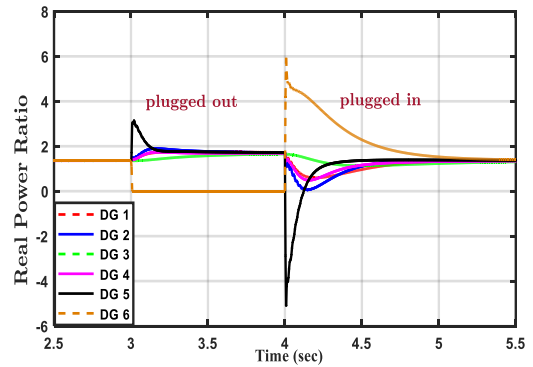


(a) method of Bidram et al. [28]

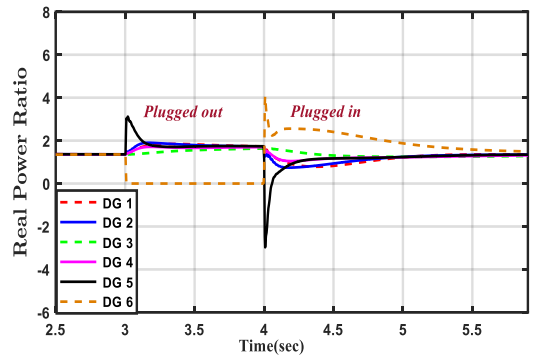


(b) the proposed method

Figure 11. DGs output frequency



(a) method of Bidram et al. [28]



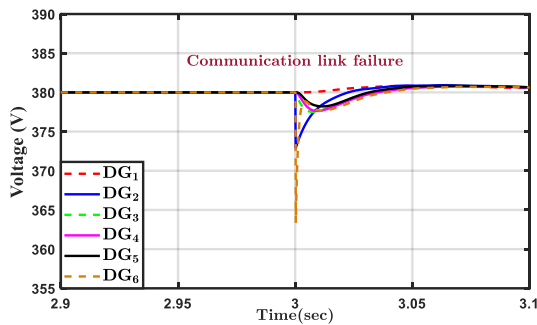
(b) the proposed method

Figure 12. DGs output real power ratio

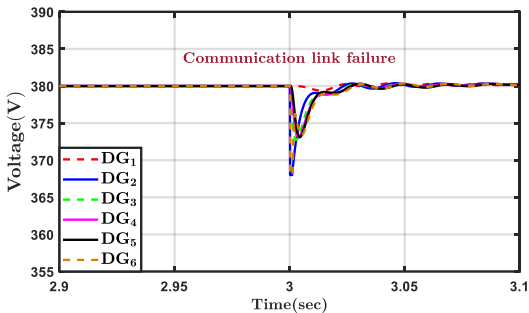
Immediately after reconnection of this link, the link between DG 5 and DG6 is disconnected for 1 m.s and then reconnected. The results are given in Figures 13(a) and 14(a) for the method of Bidram et al. [28] and 13(b) and 14(b) for the proposed method. The results depicts that under such conditions, the islanded MG is still stable and f & V restores to their nominal values, but the proposed method has much better transient response. For example, for the proposed method, voltage magnitude achieves a steady state after 10 m.s. while for the method of Bidram et al. [28], this time is 25 msec. Moreover, the

rate of frequency change obtained from [28] is 2.2 Hz/m.s while in the proposed method this parameter is equal 0.3 Hz/m.s As the figures shown, the worst behavior belongs to DG6, because this DG is the farthest one from the leader node. Remarkably, DGs and their control mechanism typically have much slower dynamics than communication systems, which commonly use low-delay, wide-bandwidth communication protocols. This is especially true for distributed control methods where each controller only communicates with its neighbors. Because of that, we do not discuss about delays in this paper.

4. 4. Case 4: DG Parameters Change In this case, the performance of the proposed ADVC is verified subsequent to the changes in network parameters. It is assumed that at $t = 1$ s, the filters capacitors are randomly changed from 49 to 51 μF . Figure 15 shows

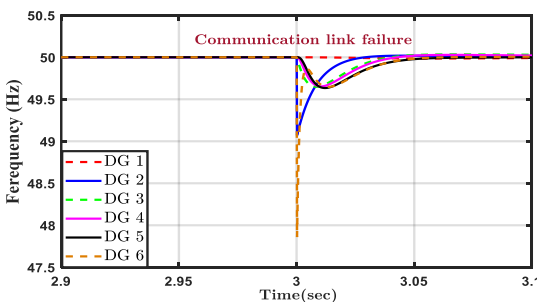


(a) method of Bidram et al. [28]

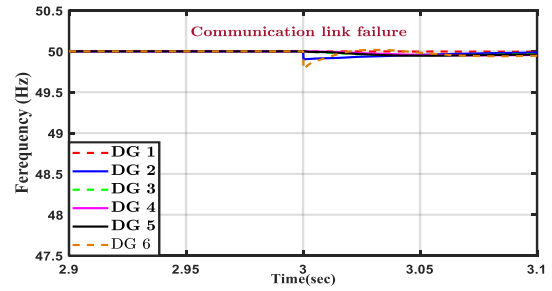


(b) the proposed method

Figure 13. DGs output voltage magnitudes in case 3



(a) method of Bidram et al. [28]



(b) the proposed method

Figure 14. DGs output frequency in case 3

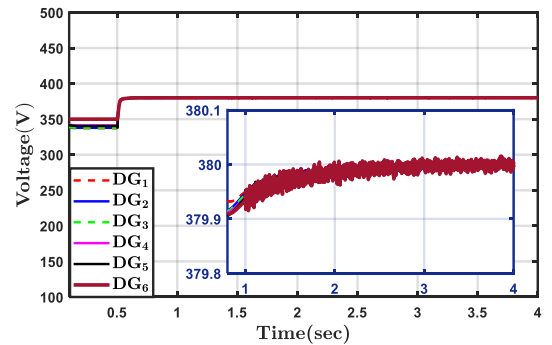


Figure 15. DGs output voltage magnitudes in case 4- The proposed protocol

the results of the output voltages of DGs over time under this condition. As the figure shows, the DGs voltages remain in the permissible range and the system tolerates that parameter changes. In fact, these changes are the events that occur in real situations due to the tolerances, temperature, aging and etc. The result shows that performance of the adaptive voltage controller does not deteriorate as a result of the changes in filter capacitors.

5. CONCLUSION AND FUTURE WORKS

Based on an adaptive fully distributed algorithm, two secondary controllers were presented in this work to improve the behavior of MGs during islanded operation. The nonlinear nature of MGs has been covered in the algorithm. In spite of other methods that require complete DGs information, in this method only the power droop coefficient is needed. A consensus-based strategy was developed to returns and to synchronize f & V of MG to their referenced values after any disruption. The stabilization of the synchronization problem was proved using a rigorous Lyapunov analysis. The effectiveness of the proposed method was examined using a typical six-DGs network. The obtaining results were compared to method introduced by Bidram and his coworkers to validate the method. The results show the efficacy of the proposed secondary controllers which are less sensitive

to intense disturbances and presents low overshoot and settling time during load changes, plug and play and communication links failure. Indeed, the proposed controllers enhance the resiliency of MGs. The proposed distributed adaptive control is very simple in terms of structure and unlike centralization methods, does not require a large and complex communication network. Also, it can be easily implemented and used in software.

Limitations and future applications: Communication is indispensable to access neighbor data and, thus, to the operation of the distributed control system. Accordingly, channel non-idealities such as communication transmission/propagation delay/noises and limited bandwidth, may compromise the overall system performance. A few aspects listed below attract the authors' interest to do research on them in future works:

- A detailed discussion about the voltage drop as a result of a communication link failure.
- The proposed secondary control scheme can be extended to address the communication network related issues, such as data loss, packet jamming, link failure, cyber attack, etc.

6. REFERENCES

1. Keshavarz, M., Doroudi, A., Kazemi, M. H., and Dehkordi, N. M., "A Novel Hybrid Droop-Isochronous Control Strategy for Microgrid Management", *Iranian Journal of Electrical and Electronic Engineering*, Vol. 17, No. 2, (2021), 1798-1798, Doi: 10.22068/IJEEE.17.2.1798.
2. Bidram, A., Poudel, B., Damodaran, L., Fierro, R., and Guerrero, J. M., "Resilient and cybersecure distributed control of inverter-based islanded microgrids", *IEEE Transactions on Industrial Informatics*, Vol. 16, No. 6, (2020) 3881-3894, Doi: 10.1109/TII.2019.2941748.
3. Lou, G., Gu, W., Sheng, W., Song, X., and Gao, F., "Distributed model predictive secondary voltage control of islanded microgrids with feedback linearization", *IEEE Access*, Vol. 6, (2018), 50169-50178, Doi: 10.1109/ACCESS.2018.2869280.
4. Dahiya, R., "Stability analysis of islanded DC microgrid for the proposed distributed control strategy with constant power loads", *Computers & Electrical Engineering*, Vol. 70, (2018), 151-162, Doi: 10.1016/j.compeleceng.2018.02.020.
5. Lavanya, V., & Senthil Kumar, N. "Seamless Transition in Grid-connected Microgrid System using Proportional Resonant Controller", *International Journal of Engineering, Transactions A: Basics*, Vol. 33, No. 10, (2020), 1951-1958. Doi: 10.5829/IJE.2020.33.10A.13.
6. Farzinfar, M., Nair, N. K. C., & Bahadornjad, M. "A New Adaptive Load-Shedding and Restoration Strategy for Autonomous Operation of Microgrids: A Real-Time Study", *International Journal of Engineering, Transactions A: Basics*, Vol. 33, No. 1, (2020), 82-91. Doi: 10.5829/IJE.2020.33.01A.10.
7. Han, Y., Zhang, K., Li, H., Coelho, E. A. A., and Guerrero, J. M. "MAS-based distributed coordinated control and optimization in microgrid and microgrid clusters: A comprehensive overview", *IEEE Transactions on Power Electronics*, Vol. 33, No. 8, (2017), 6488-6508, Doi: 10.1109/TPEL.2017.2761438.
8. Ko, B. S., Lee, G. Y., Choi, K. Y., Kim, R. Y., Kim, S., Cho, J., and Kim, S. I., "Flexible Control Structure for Enhancement of Scalability in DC Microgrids", *IEEE Systems Journal*, Vol. 14, No. 3, (2020), 4591-4601, Doi: 10.1109/JSYST.2019.2963707.
9. Sharma, R., and Sathans, S., "Virtual impedance based phase locked loop for control of parallel inverters connected to islanded microgrid", *Computers & Electrical Engineering*, Vol. 73, (2019), 58-70, Doi: 10.1016/j.compeleceng.2018.11.005.
10. Muhammad, M., Chul-Hwan, K., Muhammad, S., "Robust Centralized Control for DC Islanded Microgrid Considering Communication Network Delay", *IEEE Access*, Vol. 8, (2020), 77765-77778, Doi: 10.1109/ACCESS.2020.2989777.
11. Qian, T., Liu, Y., Zhang, W., Tang, W., Shahidepour, M., "Event-triggered updating method in centralized and distributed secondary controls for islanded microgrid restoration", *IEEE Transactions on Smart Grid*, Vol. 11, No. 2, (2019), 1387-1395, Doi: 10.1109/TSG.2019.2937366.
12. Amir, H., Markadeh, G. A., Dehkordi, N. M., and Blaabjerg, F., "decentralized robust backstepping voltage control of photovoltaic systems for DC islanded microgrid based on disturbance observer method", *ISA Transactions*, Vol. 101, (2020), 471-481, Doi: 10.1016/j.isatra.2020.02.006.
13. Arani, A. A. K., Gharehpetian, G. B., Abedi, M., "Decentralized primary and secondary control strategies for islanded microgrids considering energy storage systems characteristics", *IET Generation, Transmission & Distribution*, Vol. 13, No. 14, (2019), 2986-2992, 2019, Doi: 10.1049/iet-gtd.2019.0362.
14. Dehkordi, N. M., Moussavi, S. Z. "Distributed resilient adaptive control of islanded microgrids under sensor/actuator faults", *IEEE Transactions on Smart Grid*, Vol. 11, No. 3, (2019), 2699-2708, Doi: 10.1109/TSG.2019.2960205.
15. Peng, J., Fan, B., and Liu, W., "Voltage-Based Distributed Optimal Control for Generation Cost Minimization and Bounded Bus Voltage Regulation in DC Microgrids", *IEEE Transactions on Smart Grid*, Vol. 12, No. 1, (2020), 106-116, Doi: 10.1109/TSG.2020.3013303.
16. Espina, E., Llanos, J., Burgos-Mellado, C., Cardenas-Dobson, R., Martinez-Gomez, M., and Saez, D., "Distributed Control Strategies for Microgrids: An Overview", *IEEE Access*, Vol. 8, (2020), 193412-193448, Doi: 10.1109/ACCESS.2020.3032378.
17. Li, Z., Zang, C., Zeng, P., Yu, H., and Li, S., "Fully distributed hierarchical control of parallel grid-supporting inverters in islanded AC microgrids", *IEEE Transactions on Industrial Informatics*, Vol. 14, No. 2, (2018), 679-690, Doi: 10.1109/TII.2017.2749424.
18. Zhang, Z., Dou, C., Yue, D., Zhang, B., Xu, S., Hayat, T., and Alsaedi, A., "An event-triggered secondary control strategy with network delay in islanded microgrids", *IEEE Systems Journal*, Vol. 13, No. 2, (2018), 1851-1860.
19. Zuo, S., Altun, T., Lewis, F. L., and Davoudi, A. "Distributed resilient secondary control of DC microgrids against unbounded attacks", *IEEE Transactions on Smart Grid*, Vol. 11, No. 5, (2020), 3850-3859, Doi: 10.1109/TSG.2020.2992118.
20. Mathew, P., Madichetty, S., Mishra, S., "A multilevel distributed hybrid control scheme for islanded DC microgrids", *IEEE Systems Journal*, Vol. 13, No. 4, (2019), 4200-4207, Doi: 10.1109/JSYST.2019.2896927.
21. Li, Q., Peng, C., Wang, M., Chen, M., Guerrero, J. M., and Abbott, D., "Distributed secondary control and management of islanded microgrids via dynamic weights", *IEEE Transactions on Smart Grid*, Vol. 10, No. 2, (2018), 2196-2207. Doi: 10.1109/TSG.2018.2791398.
22. Amoateng, D. O., Al Hosani, M., Elmoursi, M. S., Turitsyn, K., and Kirtley, J. L., "Adaptive voltage and frequency control of islanded multi-microgrids", *IEEE Transactions on Power Systems*, Vol. 33, No. 4, (2017), 4454-4465, Doi: 10.1109/TPWRS.2017.2780986.

23. Wu, X., Shen, C., and Iravani, R., "A distributed, cooperative frequency and voltage control for microgrids", *IEEE Transactions on Smart Grid*, Vol. 9, No. 4, (2018), 2764-2776, Doi: 10.1109/TSG.2016.2619486.
24. Li, Z., Zang, C., Zeng, P., Yu, H., and Li, S. "Fully distributed hierarchical control of parallel grid-supporting inverters in islanded AC microgrids", *IEEE Transactions on Industrial Informatics*, Vol. 14, No. 2, 679-690, Doi: 10.1109/TII.2017.2749424.
25. Dehkordi, N. M., Sadati, N., and Hamzeh, M., "Distributed robust finite-time secondary voltage and frequency control of islanded microgrids", *IEEE Transactions on Power Systems*, Vol. 32, No. 5, (2017), 3648-3659, Doi: 10.1109/TPWRS.2016.2634085.
26. Jin, Z., Meng, L., Guerrero, J. M., and Han, R., "Hierarchical control design for a shipboard power system with DC distribution and energy storage aboard future more-electric ships", *IEEE Transactions on Industrial Informatics*, Vol. 14, No. 2, (2017), 703-714, Doi: 10.1109/TII.2017.2772343.
27. Dehkordi, N.M., Sadati, N., and Hamzeh, M., "Fully distributed cooperative secondary frequency and voltage control of islanded microgrids", *IEEE Transactions on Energy Conversion*, Vol.32, No. 2, (2016), 675-685, Doi: 10.1109/TEC.2016.2638858,
28. Bidram, A., Davoudi, A., and Lewis, F. L., "A multiobjective distributed control framework for islanded AC microgrids", *IEEE Transactions on Industrial Informatics*, Vol. 10, No. 3, (2014), 1785-1798, Doi: 10.1109/TII.2014.2326917.
29. Shahab, M. A., Mozafari, B., Soleymani, S., Dehkordi, N. M., Mohammadnezhad Shourkaei, H., and Guerrero, J. M., "Stochastic Consensus-Based Control of μ Gs With Communication Delays and Noises", *IEEE Transactions on Power Systems*, Vol. 34, No. 5, (2019), 3573-3581, Doi: 10.1109/TPWRS.2019.2905433.
30. Bidram, A., Davoudi, A., Lewis, F. L., and Guerrero, J. M., "Distributed cooperative secondary control of microgrids using feedback linearization", *IEEE Transactions on Power Systems*, Vol. 28, No. 3, (2013), 3462-3470, Doi: 10.1109/TPWRS.2013.2247071.
31. Olivares, D. E, Mehrizi-Sani, A., Etemadi, A. H., Cañizares, C. A., Iravani, R., Kazerani, M., Hajimiragha, A. H., Gomis-Bellmunt, O., Saeedifard, M., and Palma-Behnke, R., "Trends in microgrid control", *IEEE Transactions on Smart Grid*, Vol. 5, No. 4, (2014), 1905-1919, Doi: 10.1109/TSG.2013.2295514.
32. Dehkordi, N. M., Baghaee, H. R., Sadati, N., and Guerrero, J. M., "Distributed noise-resilient secondary voltage and frequency control for islanded microgrids", *IEEE Transactions on Smart Grid*, Vol. 10, No. 4, (2018). 3780-3790, Doi: 10.1109/TSG.2018.2834951.
33. Bidram, A., Davoudi, A., Lewis, F. L., and Ge, S. S., "Distributed adaptive voltage control of inverter-based microgrids", *IEEE Transactions on Energy Conversion*, Vol. 29, No. 4, (2014). 862-872, Doi: 10.1109/TEC.2014.2359934.
34. Afshari, A., Karrari, M., Baghaee, H. R., and Gharehpetian, G. B., "Distributed fault-tolerant voltage/frequency synchronization in autonomous AC microgrids", *IEEE Transactions on Power Systems*, Vol. 35, No. 5, (2020), 3774-3789, Doi: 10.1109/TPWRS.2020.2975115.
35. Qu, Z., "Cooperative control of dynamical systems: applications to autonomous vehicles", Springer Science & Business Media, (2009).
36. Lv, Y., Li, Z., and Duan, Z., "Distributed adaptive consensus protocols for multiple Lur'e systems over directed graphs", *IET Control Theory & Applications*, Vol. 10, No. 4, (2016), 443-450, Doi: 10.1049/iet-cta.2015.0682.
37. Li, Z., Wen, G., Duan, Z., and Ren, W., "Designing fully distributed consensus protocols for linear multi-agent systems with directed graphs", *IEEE Transactions on Automatic Control*, Vol. 60, No. 4, (2014), 1152-57, Doi: 10.1109/TAC.2014.2350391.
38. Zhang, H., Lewis, F. L., and Qu, Z., "Lyapunov, adaptive, and optimal design techniques for cooperative systems on directed communication graphs", *IEEE Transactions on Industrial Electronics*, Vol. 59, No. 7, (2011), 3026-6041, Doi: 10.1109/TIE.2011.2160140.
39. Bernstein, D. S., "Matrix mathematics: theory, facts, and formulas", Princeton university press, (2009).

Persian Abstract

چکیده

این مقاله یک کنترل‌کننده ثانویه تطبیقی توزیع‌شده جدید را برای میکروگریدها (MGs) در حالت عملکرد جزیره‌ای پیشنهاد می‌کند. کنترل‌کننده پیشنهادی برای بهبود رفتار دینامیکی یک میکروگرید تحت اختلالات، از ساختار کنترل تطبیقی مبتنی بر اجماع استفاده می‌کند. یک پروتکل اجماع جدید برای بازگرداندن فرکانس و ولتاژ (f & V) میکروگرید به مقادیر نامی آن‌ها و یک تابع لیاپانوف برای اطمینان از پایداری مجانبی سیستم و حد نهایی خطای همسایگی ارائه شده است. ماهیت غیرخطی میکروگرید نیز در الگوریتم پوشش داده شده است. کنترل‌کننده پیشنهادی بر خلاف روش‌های دیگر که به اطلاعات کامل ژنراتورهای توزیع‌شده (DG) نیاز دارند، فقط به اطلاعات ضرایب افت توان نیاز دارد و مستقل از پارامترهای ژنراتورهای توزیع‌شده است. شبیه‌سازی‌های مختلفی برای بررسی عملکرد کنترل‌کننده تطبیقی، در جعبه ابزار MATLAB/SimPower روی یک میکروگرید نمونه و تحت اختلالات مختلف انجام شده است. نتایج شبیه‌سازی، کارایی کنترل‌کننده پیشنهادی را در افزایش تاب آوری میکروگریدها نشان می‌دهد.
